Application of higher-order spectra for signal processing in electrical power engineering

T. LOBOS, Z. LEONOWICZ, J. SZYMANDA, P. RUCZEWSKI*

During recent years higher order statistics (HOS) have found a wide applicability in many diverse fields, e.g.: biomedicine, harmonic retrieval and adaptive filtering.
In power spectrum estimation, the signal under consideration is processed in such a way, that the distribution of power among its frequency is estimated and phase relations between the frequency components are suppressed. Higher order statistics and their associated Fourier transforms reveal not only amplitude information about a signal, but also phase information. If a non-Gaussian signal is received along with additive Gaussian noise, a transformation to higher order cumulant domain eliminates the noise.
These are some methods for estimation of signal components, based on HOS. In the paper we apply the MUSIC method both for the correlation and the 4^{th} order cumulant, to investigate the state of asynchronous running of synchronous machines and the fault operation of inverter-fed induction motors.
When the investigated signal is distorted by a coloured noise, more exact results can be achieved by applying cumulants.

Keywords: higher order statistics, spectral analysis, synchronous generators, induction motors, semiconductor inverters, fault detection.

1. Spectrum estimation methods

The linear methods of spectrum estimation (Blackman-Tukey, direct methods based on FFT) suffer from a major problem of resolution (Naidu, 1996). Because of some invalid assumptions (zero data or repetitive data outside the duration of observation) made in these methods, the estimated spectrum will be a smeared version of the true spectrum. Closely spaced spectral peaks get merged into a broader peak, leading to false estimates of spectral power. Even the best window becomes ineffective when the dynamic range of the spectrum is high. Methods using a data adaptive window (ML, Capon), invented to alleviate this problem, deliver high resolution at moderate SNR only.

If we are able to extrapolate the available data outside the duration of the data (it means to fit the data with a finite rational model), we can completely eliminate the use of the window itself. Once the model parameters are estimated, the spectrum may be derived from the model parameters or from the extrapolated data. The most important time series models are: AR(autoregressive), MA (moving average) and ARMA.

The most recent methods of spectrum estimation are based on the linear algebraic concepts of subspaces and so have been called "subspace methods" (Therrien, 1992). Its resolution is theoretically independent of the SNR. The model of the signal in this case is a sum of random sinusoids in the background of noise of a known covariance function. Pisarenko first observed that the zeros of the z-transform of the eigenvector corresponding to the minimum eigenvalue of the covariance matrix lie on the unit circle, and their angular positions correspond to the frequencies of the sinusoids. In a later development it was shown that the eigenvectors may be divided into two groups, namely, the eigenvectors spanning the signal space and eigenvectors spanning the orthogonal noise space. The eigenvectors spanning the noise space are the ones whose eigenvalues are the smallest and equal to the noise power. One of the most important techniques, based on the Pisarenko's approach of separating the data into signal and noise subspaces, is the MUSIC method.

2. MUSIC (MUltiple SIgnal Classification)

The MUSIC method (Therrien, 1992) involves projection of the signal vector:

$$\mathbf{s}_i = \begin{bmatrix} 1 & e^{j\omega_i} & \cdots & e^{j(N-1)\omega_i} \end{bmatrix}^T \tag{1}$$

onto the entire noise subspace.

We consider a random sequence **x** made up of *M* independent signals in noise.

$$\mathbf{x} = \sum_{i=1}^{M} A_i \mathbf{s}_i + \eta\,; \quad A_i = |A_i| e^{j\phi_i} \tag{2}$$

* Wroclaw University of Technology, pl. Grunwaldzki 13, 50-370 Wroclaw, Poland

$$\text{or: } \mathbf{x} = \mathrm{S}\begin{bmatrix} A_1 & A_2 & \cdots & A_M \end{bmatrix}^T + \eta \tag{3}$$

$$\text{where } \mathbf{S} = \begin{bmatrix} \mathbf{s}_1 & \mathbf{s}_2 & \cdots & \mathbf{s}_M \end{bmatrix}$$

(general model used in all "subspace methods"). If the noise (η) is white, the correlation matrix is

$$\mathbf{R}_x = \sum_{i=1}^{M} E\left\{ A_i A_i^* \right\} \mathbf{s}_i \mathbf{s}_i^T + \sigma_0^2 \mathbf{I} \tag{4}$$

$$\text{or: } \mathbf{R}_x = \mathbf{S}\mathbf{P}_0\mathbf{S}^{*T} + \sigma_0^2 \mathbf{I} \tag{5}$$

$$\text{where } \mathbf{P}_0 = \begin{bmatrix} E\left\{ A_1 A_1^* \right\} & 0 & \cdots & 0 \\ 0 & E\left\{ A_2 A_2^* \right\} & \cdots & 0 \\ \vdots & \vdots & \ddots & 0 \\ 0 & 0 & \cdots & E\left\{ A_M A_M^* \right\} \end{bmatrix}$$

N-M smallest eigenvalues of the correlation matrix (matrix dimension *N*>*M*+1) correspond to the noise subspace and *M* largest (all greater than σ_0^2) corresponds to the signal subspace.

We define the matrices of eigenvectors:

$$\mathbf{E}_{signal} = \begin{bmatrix} \mathbf{e}_1 & \mathbf{e}_2 & \cdots & \mathbf{e}_M \end{bmatrix} \tag{6}$$

$$\mathbf{E}_{noise} = \begin{bmatrix} \mathbf{e}_{M+1} & \mathbf{e}_{M+2} & \cdots & \mathbf{e}_N \end{bmatrix} \tag{7}$$

and also two matrices of eigenvalues:

$$\mathbf{\Lambda}_{signal} = \begin{bmatrix} \lambda_1 & 0 & \cdots & 0 \\ 0 & \lambda_2 & \cdots & 0 \\ \vdots & \vdots & \ddots & \vdots \\ 0 & 0 & \cdots & \lambda_M \end{bmatrix} \tag{8}$$

$$\mathbf{\Lambda}_{noise} = \begin{bmatrix} \lambda_{M+1} & 0 & \cdots & 0 \\ 0 & \lambda_{M+2} & \cdots & 0 \\ \vdots & \vdots & \ddots & \vdots \\ 0 & 0 & \cdots & \lambda_N \end{bmatrix} = \begin{bmatrix} \sigma_0^2 & 0 & \cdots & 0 \\ 0 & \sigma_0^2 & \cdots & 0 \\ \vdots & \vdots & \ddots & \vdots \\ 0 & 0 & \ldots & \sigma_0^2 \end{bmatrix}$$

It is possible to write $\mathbf{R}_x$ as:

$$\mathbf{R}_x = \mathbf{E}_{signal}\mathbf{\Lambda}_{signal}\mathbf{E}_{signal}^{*T} + \mathbf{E}_{noise}\mathbf{\Lambda}_{noise}\mathbf{E}_{noise}^{*T} \tag{9}$$

$\mathbf{E}_{noise}$ can be used to form a projection matrix $\mathbf{P}_X$ for the noise subspace

$$\mathbf{P}_{noise} = \mathbf{E}_{noise}\mathbf{E}_{noise}^{*T} = \mathbf{I} - \mathbf{P}_{signal} \tag{10}$$

The squared magnitude of the projection of **w** (defined as in (1)) onto the noise subspace is given by

$$\mathbf{w}^{*T}\mathbf{P}_{noise}\mathbf{w} = \mathbf{w}^{*T}\mathbf{E}_{noise}\mathbf{E}_{noise}^{*T}\mathbf{w} \tag{11}$$

Since each of the elements of the signal vector is orthogonal to the noise subspace, the quantity (11) goes to zero for values of the frequency where $\mathbf{w}=\mathbf{s}_i$.

The MUSIC pseudospectrum is defined as

$$\hat{P}\left(e^{j\omega}\right) = \left[\mathbf{w}^{*T}\mathbf{P}_{noise}\mathbf{w}\right]^{-1} = \left[\mathbf{w}^{*T}\mathbf{E}_{noise}\mathbf{E}_{noise}^{*T}\mathbf{w}\right]^{-1} \tag{12}$$

and it exhibits sharp peaks at the signal frequencies where $\mathbf{w}=\mathbf{s}_i$.

An alternative variation of the method of pseudospectrum estimation can be developed as follows. Define the eigenfilter

$$E_i(z) = e_i[0] + e_i[1]z^{-1} + \ldots + e_i[N-1]z^{-(N-1)} \tag{13}$$

where $e_i[n]$ are components of the eigenvector $\mathbf{e}_i$. The equation (11) can be written using (13) as

$$\sum_{i=M+1}^{N} \mathbf{w}^{*T}\mathbf{e}_i\mathbf{e}_i^{*T}\mathbf{w} = \sum_{i=M+1}^{N} E_i\left(e^{j\omega}\right) E_i^*\left(e^{j\omega}\right) \tag{14}$$

The MUSIC pseudospectrum can therefore be expressed as

$$\hat{P}\left(e^{j\omega}\right)=\left[\sum_{i=M+1}^{N}E_i(z)E_i^*\left(1/z^*\right)\right]^{-1}\Bigg|_{z=e^{j\omega}} \tag{15}$$

The denominator polynomial (15) has M double roots lying on the unit circle, which correspond to the signal frequencies.

If the frequencies are to be found by *plotting* the pseudospectrum, then the spectrum can be written in the form

$$\hat{P}\left(e^{j\omega}\right)=\left[\sum_{i=M+1}^{N}\left|\mathbf{w}^{*T}\mathbf{e}_i\right|^2\right]^{-1} \tag{16}$$

Let the components of the vector $\mathbf{e}_i$ be regarded as a sequence $e_i[0]$, $e_i[1]$,..., $e_i[N\text{-}1]$. Then the Fourier transform of this sequence is

$$E_i\left(e^{j\omega}\right)=\mathbf{w}^{*T}\mathbf{e}_i \tag{17}$$

The L values of (17) corresponding to the L desired frequency points can be found by zero-padding the sequence $e_i[n]$ to a length L and using an L-point FFT. A total of N such FFT's is needed to evaluate (16).

In the most common situation where the number of signals is not known at the outset, it must be estimated from the data. When the SNR is high, it is easy to determine M from the inspection of the eigenvalues. In other cases the AIC (Akaike Information Criterion) or the MDL (Minimum Description Length) are useful.

$$AIC(M)=-2K(N-M)\ln\rho(M)+2M(2N-M) \tag{18}$$

$$MDL(M)=-K(N-M)\ln\rho(M)+\tfrac{1}{2}M(2N-M)\ln K \tag{19}$$

$$\text{where: } \rho(M)=\frac{\left(\lambda_{M+1}\cdot\lambda_{M+2}\cdot\ldots\cdot\lambda_N\right)^{\frac{1}{N-M}}}{\frac{1}{N-M}\left(\lambda_{M+1}+\lambda_{M+2}+\ldots+\lambda_N\right)} \tag{20}$$

(K-number of rows of the data matrix). The value of M is chosen to minimise (18) or (19).

3. Cumulant-based approach

The second-, third-, and fourth-order cumulants of a zero-mean stationary random process $x(t)$ are

$$C_{1,x}=E\{x(t)\}=0 \tag{21}$$

$$C_{2,x}(\tau)=E\{x(t)x(t+\tau)\} \tag{22}$$

$$C_{3,x}(\tau_1,\tau_2)=E\{x(t)x(t+\tau_1)x(t+\tau_2)\} \tag{23}$$

$$\begin{aligned}C_{4,x}(\tau_1,\tau_2,\tau_3)=&E\{x(t)x(t+\tau_1)x(t+\tau_2)x(t+\tau_3)\}+\\&-C_{2,x}(\tau_1)C_{2,x}(\tau_2-\tau_3)-C_{2,x}(\tau_2)C_{2,x}(\tau_3-\tau_1)+\\&-C_{2,x}(\tau_3)C_{2,x}(\tau_1-\tau_2)=cum(\ldots)\end{aligned} \tag{24}$$

There are many signal processing applications where signals are either real or complex (sinusoidal) processes. This general class of signals can be described by

$$x(n)=\sum_{i=1}^{p}a_i(n)s_n(\omega_i) \tag{25}$$

where $s_n(.)$ are signal waveshapes, ω_i are constants and $a_i(n)$'s are random variables.

In case of complex harmonic processes (25) can be expressed as (Mendel, 1991)

$$x(n)=\sum_{i=1}^{p}\alpha_i\exp\left[j(\omega_i n+\phi_i)\right] \tag{26}$$

where ϕ_i are independent identically distributed random variables uniformly distributed over $[0, 2\pi]$, $\omega_i\neq\omega_j$ for $i\neq j$ and α_i's i ω_i's are constants.

The comparable model for real signals is

$$y(n) = \sum_{i=1}^{p} \alpha_i \cos\left(\omega_i n + \phi_i\right) \tag{27}$$

For random variables $b=e^{j\psi}$, where ψ is uniformly distributed over $[0, 2\pi]$, was shown the following.

1) All third-order cumulants of complex harmonic b are always zero.
2) Of the three different ways to define a fourth-order cumulant of a complex harmonic only one always yields a nonzero value , i.e., $cum(b, b, b, b)=0$, $cum(b^*, b, b, b)=0$ but $cum(b^*, b^*, b, b)= -1$.

For (26) in the case of complex harmonics the fourth-order cumulant is given by

$$C_{4,x}\left(\tau_1, \tau_2, \tau_3\right) = -\sum_{k=1}^{p} \alpha_k^4 \exp\left[j\omega_k\left(-\tau_1 + \tau_2 + \tau_3\right)\right] \tag{28}$$

For (27) in the case of real harmonics

$$\begin{aligned} C_{4,x} = -\tfrac{1}{8}\sum_{k=1}^{p} \alpha_k^4 \Big[&\cos\omega_k\left(\tau_1 - \tau_2 - \tau_3\right) + \cos\omega_k\left(\tau_2 - \tau_3 - \tau_1\right) + \\ &+ \cos\omega_k\left(\tau_2 - \tau_3 - \tau_1\right)\Big] \end{aligned} \tag{29}$$

$$\text{Additionally, } C_{2,x} = \tfrac{1}{2}\sum_{k=1}^{p} \alpha_k^2 \cos\left(\omega_k \tau\right) \tag{30}$$

If $x(n)$ is a sum of p real-valued sinusoids, then the diagonal slice of the fourth-order cumulant retains all of the pertinent information about the number of harmonics, their amplitudes and frequencies (Mendel, 1991). Especially set $\tau_1 = \tau_2 = \tau_3 = \tau$ in (29) to see that

$$C_{4,y}(\tau) = -\tfrac{3}{8}\sum_{k=1}^{p} \alpha_k^4 \cos\left(\omega_k \tau\right) \tag{31}$$

which is nearly identical with the autocorrelation of the signal.

It is known that signal parameters can be estimated from the output correlation in the white noise case, they can also be estimated from the fourth-order cumulant, which is useful in the additive coloured noise case. It means that existing high-resolution methods, such as MUSIC, can be applied by replacing correlation quantities with fourth-order cumulant (Swami, 1991).

4. Experimental section

4.1. Asynchronous running of synchronous generators

When a fault occurs at the terminals of a synchronous generator the power output of the machine is reduced but the input power from the turbine doesn't change during the short time of the fault and the rotor gains speed to store the excess energy. If the fault persists long enough, the rotor angle will increase continuously and the synchronism will be lost. After switching off the fault the current waveforms contain three main components with frequencies that depend on the rotor slip.

Assuming a steady-state asynchronous running of a synchronous machine (s=const) the stator winding current can be expressed (Kosty³a, 1994).

$$i_s = I_f \cos\left(\omega_s t + \gamma_f\right) + I_b \cos\left[(1-2s)\omega_s t + \gamma_b\right] + I_r \cos\left[(1-s)\omega_s t + \gamma_r\right] \tag{32}$$

where I_f, γ_f - amplitude and phase angle of the forward field component, I_b, γ_b - amplitude and phase angle of the backward field component, I_r, γ_r - amplitude and phase angle of the rotor field component, s - rotor slip, ω_s - angular velocity of the rotating stator field.

At the beginning of an asynchronous running, differences between frequencies are small and their identification is rather difficult.

Experimental setup

A small synchronous generator running at 47 Hz was switched on the 50 Hz power supply. The stator winding current samples (f_s=1000 Hz)(Fig. 1) were analysed with the help of the MATLAB® (v.4.2c.1) function *harmest*

(toolbox *hosa* v.2.0). Coloured noise, generated by passing white Gaussian noise through a FIR filter [1,1], was added artificially (Fig. 3).

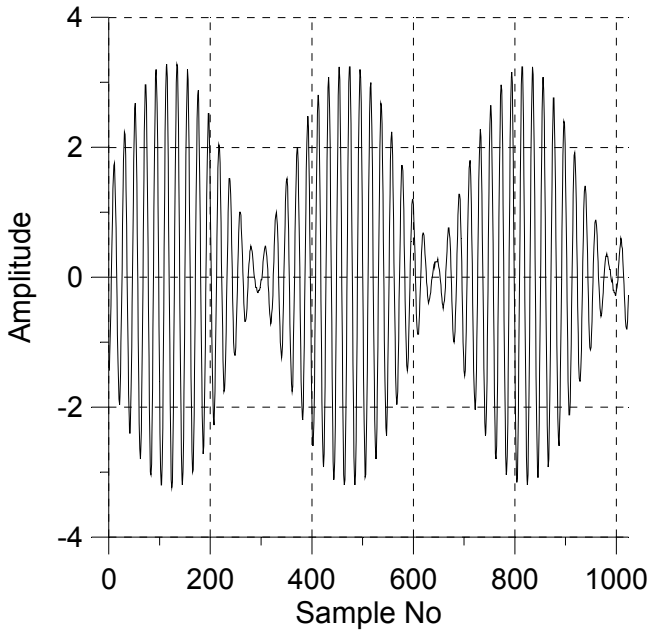

Fig. 1. Waveform of the stator winding current.

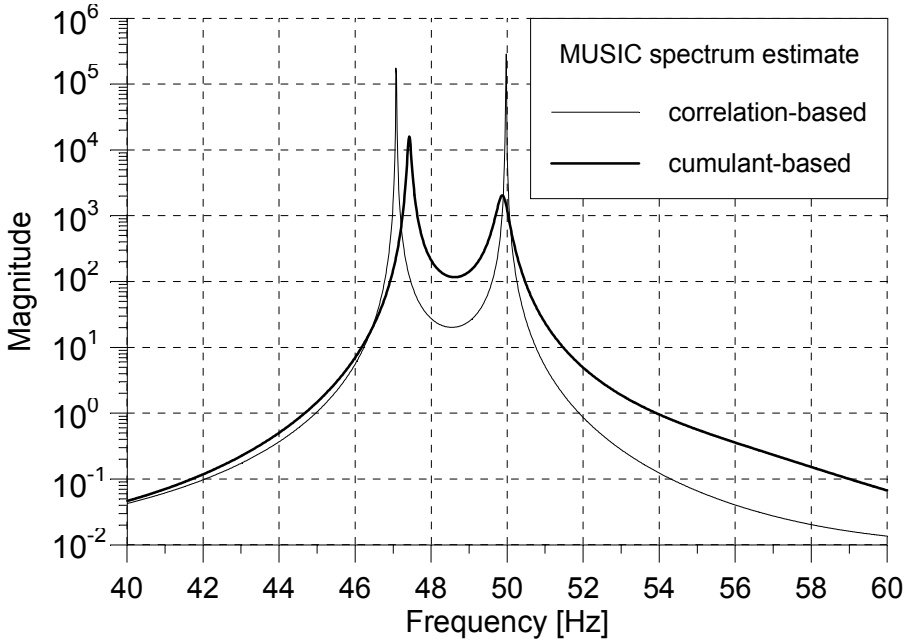

Fig. 2. MUSIC spectrum estimates in noiseless case.

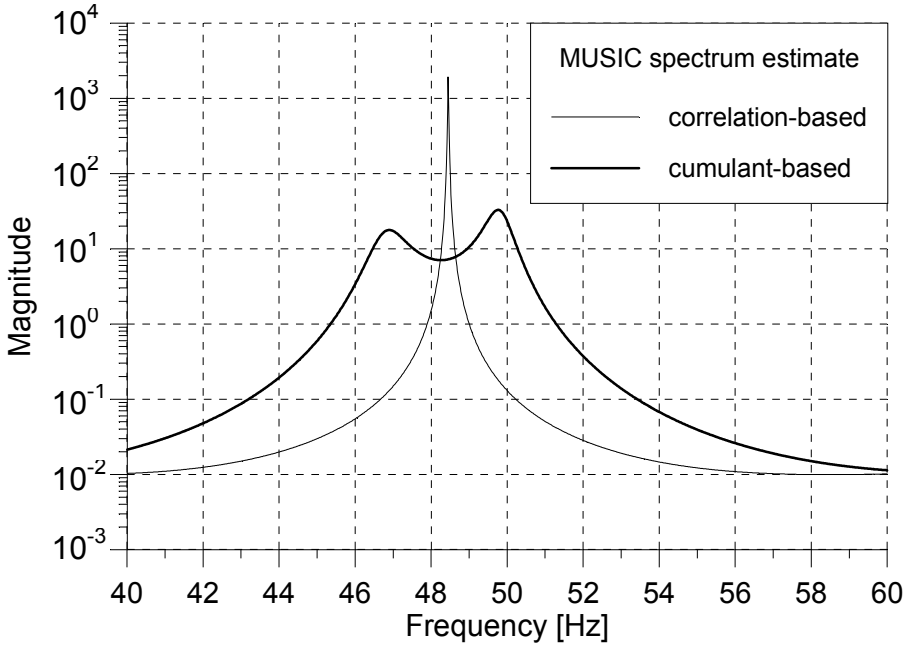

Fig. 3. MUSIC spectrum estimates in coloured noise case (SNR=0 dB) .

Table 1. Estimated signal frequencies.

	Fig. 2		Fig. 3	
	corr.	cum.	corr.	cum.
f_1 [Hz]	47.09	47.44	48.46	46.91
f_2 [Hz]	49.99	49.88	-	49.77

From the analysis it follows that the waveform of the stator current (Fig. 1) can be decomposed (resolved) into two sinusoidal components of frequencies 47 Hz and 50 Hz. Under noiseless or high-SNR conditions (Fig. 2) the correlation-based frequency estimates are more accurate (Table 1). Under poor SNR conditions only cumulant-based methods identify the correct number of signal components (Fig. 3).

4.2 Fault operations of inverter-fed induction motor drives

Fault operations of inverter-fed induction motors have been also investigated. The investigated drive represents a typical configuration of industrial AC drives, consisting of three-phase asynchronous motor an a power converter composed by a single-phase half-controlled bridge rectifier and a voltage source inverter.

The waveforms of the inverter input current (Fig. 4) under various operation conditions, taken from experimental test (Gentile, 1996), have been investigated using the correlation-based and the cumulant-based method. The main frequency at the inverter output was 40 Hz. Under normal conditions (Fig. 5) regular frequencies 240, 480, 720 and 960 Hz have been observed. Under fault conditions (switch failure) irregular frequencies 680 and 760 Hz have also been detected. The cumulant-based method shows a better accuracy and resolution than the correlation-based method.

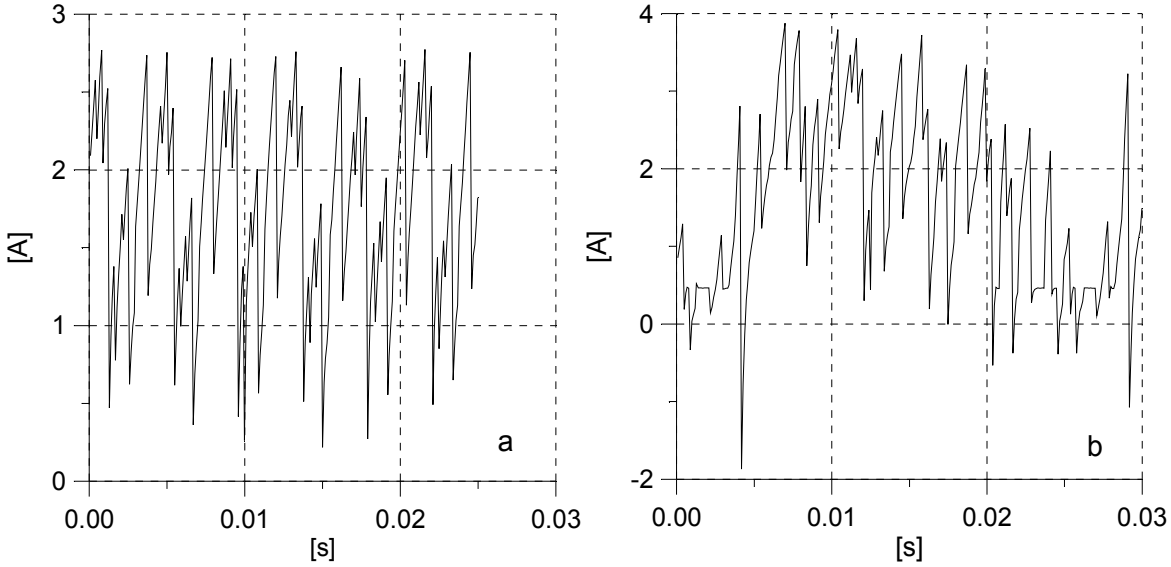

Fig. 4. Inverter input current. a) without fault b) switch failure.

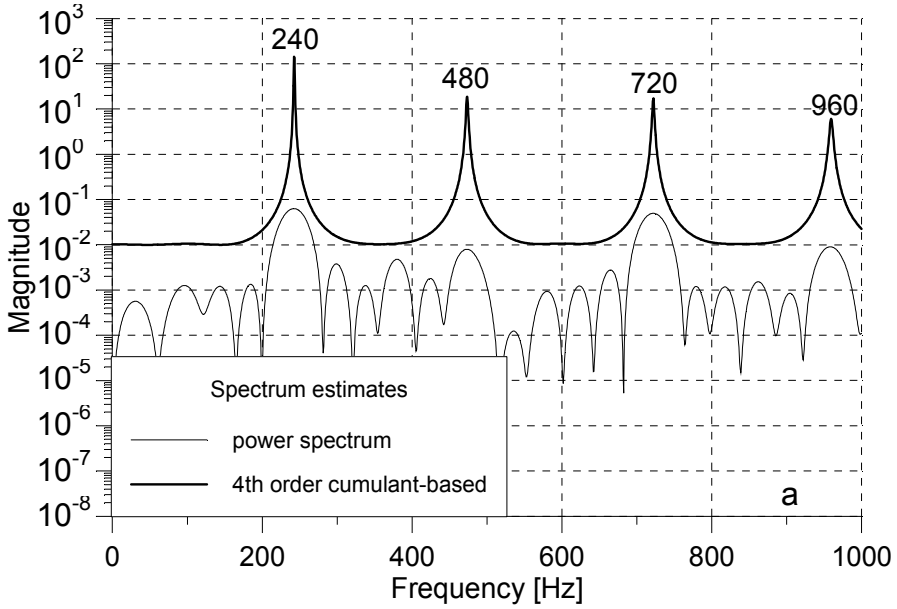

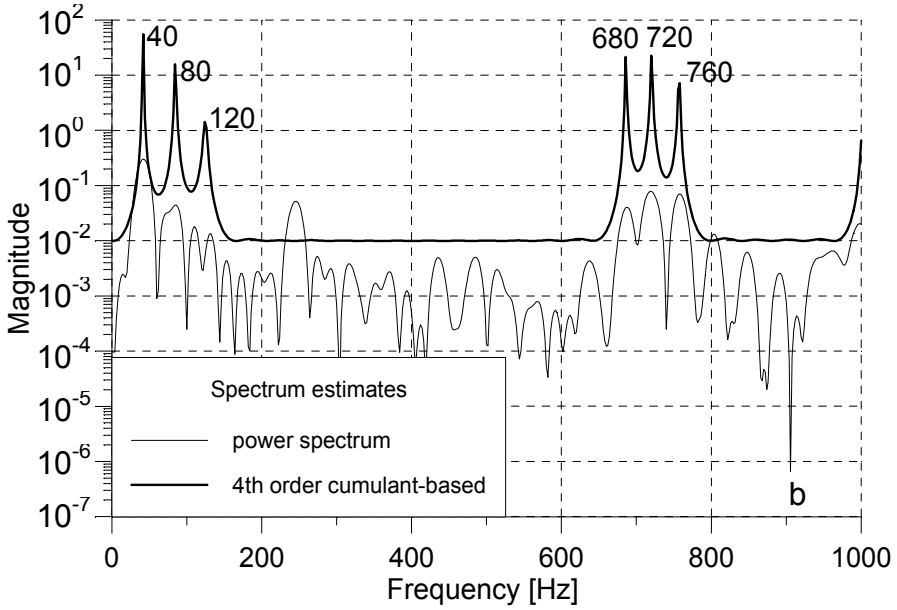

Fig. 5. Higher order spectrum estimates calculated by MUSIC method. a)without fault b)switch failure.

5. Conclusions

In the paper it was shown that high-resolution spectrum estimation methods, such as MUSIC, can be effectively used to identify the loss of synchronism of synchronous machines. Under high-SNR conditions, correlation- and cumulant-based results are similar, although cumulant-based estimates show more variability and require approximately two times longer computation times that those correlation-based. Under poor SNR conditions, when the additive Gaussian noise is coloured, only cumulant-based methods indicate the correct number of signal components.

When investigating the waveforms of the inverter input current of a inverter-fed AC drive, the cumulant-based method shows a better accuracy and resolution than the correlation-based method.

REFERENCES

GENTILE G., ROTONDALE N., TURSINI M., FRANCESCHINI G., TASSONI C., 1996, Fault operations of inverter-fed induction motor. *Proceedings of the 31st Universities Power Engineering Conference*, **2**, 353-360.

KOSTYLA P., LOBOS T., WACLAWEK Z. and PYTEL J., 1994, Identification of Asynchronous Running of Synchronous Machines using a Neural Network, *XVII Seminar on Fundamentals of Electrotechnics and Circuit Theory*, **2**, 497-502.

MENDEL J.M., 1991, Tutorial on Higher-Order Statistics (Spectra) in Signal Processing and System Theory: Theoretical Results and Some Applications, *Proceedings of the IEEE*, **79**, 278-305.

NAIDU P. S., 1996, *Modern Spectrum Analysis of Time Series* (Boca Raton: CRC Press), 241-336.

SWAMI A., 1991, Cumulant-Based Approach to the Harmonic Retrieval and Related Problems, *IEEE Transactions on Signal Processing*, **39**, 1099-1108.

THERRIEN C.W., 1992, *Discrete Random Signals and Statistical Signal Processing* (Englewood Cliffs: Prentice-Hall), 614-655.